Atmos. Chem. Phys. Discuss., 4, 2379–2403, 2004
www.atmos-chem-phys.org/acpd/4/2379/
SRef-ID: 1680-7375/acpd/2004-4-2379
© European Geosciences Union 2004

Atmospheric Chemistry and Physics Discussions

Absolute absorption cross-section and photolysis rate of I_2

A. Saiz-Lopez[1], **R. W. Saunders**[1], **D. M. Joseph**[1], **S. H. Ashworth**[2], and **J. M. C. Plane**[1]

[1]School of Environmental Sciences, University of East Anglia, Norwich, UK
[2]School of Chemical Sciences and Pharmacy, University of East Anglia, Norwich, UK

Received: 23 February 2004 – Accepted: 8 April 2004 – Published: 5 May 2004

Correspondence to: J. M. C. Plane (j.plane@uea.ac.uk)

Abstract

Following recent observations of molecular iodine (I_2) in the coastal marine boundary layer (MBL) (Saiz-Lopez and Plane, 2004), it has become important to determine the absolute absorption cross-section of I_2 at reasonably high resolution, and also to evaluate the rate of photolysis of the molecule in the lower atmosphere. The absolute absorption cross-section (σ) of gaseous I_2 at room temperature and pressure (295 K, 760 Torr) was therefore measured between 182 and 750 nm using a Fourier Transform spectrometer at a resolution of 4 cm^{-1} (0.1 nm at λ=500 nm). The maximum absorption cross-section in the visible region was observed at λ=533.0 nm to be $\sigma=(4.84\pm0.60)\times10^{-18}$ cm^2 molecule^{-1}. The spectrum is available as supplementary material accompanying this paper. The photo-dissociation rate constant (J) of gaseous I_2 was also measured directly in a solar simulator, yielding $J(I_2)=0.12\pm0.03\ \text{s}^{-1}$ for the lower troposphere. This agrees well with the value of $0.15\pm0.03\ \text{s}^{-1}$ calculated using the measured absorption cross-section, terrestrial solar flux for clear sky conditions and assuming a photo-dissociation yield of unity. A two-stream radiation transfer model was then used to determine the variation in photolysis rate with solar zenith angle (SZA), from which an analytic expression is derived for use in atmospheric models. Photolysis appears to be the dominant loss process for I_2 during daytime, and hence an important source of iodine atoms in the lower atmosphere.

1. Introduction

Over the past two decades, there has been a growing interest in the role that iodine chemistry plays in a number of atmospheric processes, in particular the iodine-catalysed destruction of O_3 in the troposphere (e.g. Jenkin et al., 1985; Chatfield and Crutzen, 1990; Davis et al., 1996; McFiggans et al., 2000). Furthermore, catalytic cycles involving chlorine and bromine appear not to be sufficient to explain O_3 depletion in the lower stratosphere at low latitudes, leading to speculation that iodine also plays a role in stratospheric chemistry (Solomon et al., 1994). Iodine may also be central to other atmospheric phenomena, including new particle formation in marine environments (O'Dowd et al., 2002a, b; Mäkelä et al., 2002) and the enhancement of halogen / inter-halogen release via uptake on sea-salt aerosol (Vogt et al., 1999; McFiggans et al., 2002).

The primary source of iodine in the atmosphere has been postulated to be the evasion of biogenic iodocarbons from the sea surface (Carpenter, 2003a; Carpenter et al., 2003b). CH_3I, CH_2I_2, CH_2IBr and CH_2ICl have all been detected in coastal environments, with emissions showing a direct correlation with tidal height and high solar irradiance (Carpenter et al., 1999, 2001). In terms of the open ocean, evaporation of iodine from the water surface, via oxidation of iodide ions in seawater under solar irradiation, has also been suggested (Miyake and Tsunogai, 1963). An alternative mechanism for the liberation of iodine from seawater involves the reaction of iodide and iodate species with atmospheric O_3 (Garland and Curtis, 1981).

The recent detection of molecular iodine at Mace Head, Ireland by differential optical absorption spectroscopy (DOAS), suggests that I_2 may also make a significant contribution to the overall iodine budget in the atmosphere (Saiz-Lopez and Plane, 2004). I_2 was found at parts per trillion (ppt) levels in the coastal marine boundary layer (MBL), with a marked increase in concentration around low tide. This correlation between I_2 production and tidal height suggests an oxidative stress mechanism within exposed macro-algal beds as the probable source of I_2 in the coastal MBL.

In the troposphere, I atom production takes place through photo-dissociation of iodocarbons ($RI/R'I_2$)

$$RI + h\nu \rightarrow R + I \quad \text{or} \quad R'I_2 + h\nu \rightarrow R'I + I. \tag{R1}$$

Photolysis of I_2 in the atmosphere will also generate I atoms through the following channels,

$$I_2 + h\nu \rightarrow I_2^* + M \rightarrow I + I + M \quad \text{collisional dissociation} \quad (M{=}N_2 \quad \text{or} \quad O_2) \tag{R2a}$$

$$\rightarrow I_2^* \rightarrow 2I \quad \text{spontaneous pre-dissociation,} \tag{R2b}$$

where I_2^* is an electronically excited iodine molecule.

The subsequent reaction of I atoms with atmospheric O_3 leads to the formation of iodine monoxide (IO), which regenerates I atoms on photolysis,

$$I + O_3 \rightarrow IO + O_2 \tag{R3}$$

$$IO + h\nu \rightarrow I + O \tag{R4}$$

or participates in iodine-catalysed O_3 destruction cycles through reactions with HO_2 (forming HOI), NO_2 (forming $IONO_2$) or halogen oxides (Jenkin et al., 1985; Davis et al., 1996; McFiggans et al., 2000). The IO self-reaction has also been identified as an important process leading to the homogeneous nucleation of MBL aerosol. New particle formation is thought to occur via the polymeric build-up of iodine oxide aerosol formed by reactions of the iodine dioxide (OIO) radical, one of the products from the self-reaction of IO (Bloss et al., 2001; Hoffmann et al., 2001; Jimenez et al., 2003).

The visible-infrared spectrum of I_2 has been the subject of numerous previous studies (Rabinowitch and Wood, 1936a; Goy and Pritchard, 1964; Ogryzlo and Thomas, 1965; Brewer and Tellinghuisen, 1972; Tellinghuisen, 1973). I_2 has a well-defined absorption structure in the visible region of the spectrum corresponding to the B←X electronic transition (Calvert and Pitts, 1966; Tellinghuisen, 1973). Photolysis in the visible region can proceed through two channels (Okabe, 1978):

$$I_2 + h\nu \rightarrow I + I^* \quad (\text{via } B^3\Pi(O_u^+)) \tag{R5a}$$

$$I_2 + h\nu \rightarrow I + I \quad (\text{via } A^3\Pi(1_u)), \tag{R5b}$$

where I represents a ground state atom $I(^2P_{3/2})$ and I^* denotes a meta-stable $I(^2P_{1/2})$ atom. Subsequent relaxation from the meta-stable state to the ground state occurs through quenching processes or radiative decay (τ~50 ms, Okabe, 1978):

$$I^*\left(^2P_{1/2}\right) \rightarrow I\left(^2P_{3/2}\right) \tag{R6}$$

Notwithstanding this earlier work, a sufficiently high resolution absolute absorption cross-section for I_2 suitable for DOAS retrievals, and a measured rate of I_2 photolysis (appropriate for atmospheric modelling), do not appear to be available in the literature.

In this paper we will describe a measurement of the absolute absorption cross-section of I_2 from the vacuum ultra-violet to the near infra-read. The photolysis rate of I_2, determined directly in a solar simulator, will then be compared with values calculated using the measured absorption spectrum and single and two-stream radiation models.

2. Experimental

2.1. Cross-section determination

The I_2 spectrum was recorded using a Fourier Transform (FT) spectrometer (Bruker, Model IFS/66). Iodine crystals (Lancaster, 99.5%) were placed in an optical cell and allowed to equilibrate at room temperature (295 K) and pressure (760 Torr of air) before each measurement was made. The spectrum was recorded in three overlapping regions: 182–500 nm, GaP diode detector, Deuterium light source; 260–555 nm, GaP diode detector, Tungsten lamp; 500–1100 nm, Si diode, Tungsten lamp. A CaF_2 beam-splitter was used in each case. All measurements were made at a resolution of 4 cm^{-1} (0.1 nm at λ=500 nm).

In order to calculate the absolute cross-section of I_2 from its absorption spectrum, an accurate measurement of the vapour pressure of I_2 is required. However, available data is sparse (see below), and so a new measurement was performed. Iodine crystals were placed in a 1/4″ stainless steel U-tube, which was sealed at one end by a pair of Baratron pressure transducers, with 0–1000 Torr and 0–10 Torr ranges. The other end of the tube was attached to a vacuum line incorporating a diffusion pump, from which the tube could be isolated by a valve. The U-tube was immersed in water, in order to maintain it at a constant ambient temperature. The temperature of the water was monitored using a K-type thermocouple and was essentially constant (<0.4 K variation) over the duration of the experiment.

The vapour pressure of the iodine was measured by first evacuating the tube as far as possible, then isolating it from the vacuum line and allowing the pressure to rise until it reached a constant value. This procedure was repeated until a consistent final pressure was observed. The vapour pressure of I_2 at 295 K was found to be 0.225±0.020 Torr, equivalent to a vapour concentration of $(7.4\pm0.7)\times10^{15}$ molecules cm^{-3}. This value is consistent with the vapour pressure of 0.30 Torr at 298 K from the JANAF Tables (Chase, 1998). In addition, our value compares very well with a pressure of 0.24 Torr evaluated from the measured data reported by Baxter et al. (1907), empirically fitted by Baxter and Grose (1915), and used by Shirley and Giauque (1959) in their measurements of thermodynamic properties of iodine.

2.2. Rate of photolysis of I_2

Figure 1 is a schematic diagram of the experimental set-up used. An excess of O_3 ($>1\times10^{16}$ molecules cm^{-3}), produced from an O_2 flow through a corona-discharge, was used to ensure that the dominant loss process of I atoms was reaction with O_3 ($k_{295\,K}(I+O_3\rightarrow IO+O_2)=1.2\times10^{-12}$ cm^3 molecule^{-1} s^{-1}; De More et al., 1997). Under these conditions, I atom recombination in the gas phase and on the cell walls was negligible. I_2 vapour was generated by maintaining a steady low flow (5–10 standard cm^{3}min^{-1}) of N_2 across a few iodine crystals in a glass trap. The reaction took place in a glass cell (length=25 cm, volume≈150 cm^3) onto which quartz windows were mounted at each end to allow for irradiation by the light source and measurement of the light intensity. Flows of N_2 (250–300 standard cm^{3}min^{-1}) were also passed across each cell window to prevent any build-up of solid product on the window surfaces. The total gas flow through the cell produced a gas residence time of 12.5±2.5 s.

Light from a "solar simulator" (Oriel Instruments, Model 91191), which employs a

1000 W Xenon lamp with an air-mass optical filter to simulate the solar irradiance between 350 and 750 nm (λ_{max}=583 nm), was directed through the cell. A condenser lens was used to ensure that the cell windows were illuminated completely with near-uniform light intensity. Neutral density filters were used to attenuate the light intensity, which was measured with a calibrated radiometer (Ramsden Scientific Instruments 550).

Downstream of the photolysis cell, the gas flowed through a 1 m-long cell fitted with quartz windows, which was used to monitor I_2 by absorption of the 546 nm emission line from a low pressure Hg lamp ($\sigma_{546\,nm}=3.9\times10^{-18}$ cm^2 molecule^{-1}, from this study). A monochromator (Optometrics, Model MC1-02, 1.2 nm resolution), with a side-on photomultiplier (Hamamatsu Photonics, Model H7710-12) and picoammeter allowed the I_2 concentration to be determined from its measured absorbance over the range 0.01 to 0.08, with a precision of ±5%. Both the photolysis cell and the absorption cell were covered with black cloth to minimise the effects of the laboratory lights.

3. Results and discussion

3.1. I_2 absorption cross-section

The absorption cross-section of I_2 from 182 to 750 nm is shown in Fig. 2. The 182–499 nm region is dominated by the Cordes bands ($D^1\Sigma_u^+ \leftarrow X^1\Sigma_g^+$) between 182 and 200 nm. This spectral region is clearly irrelevant with respect to photolysis in the lower troposphere, where only solar radiation at $\lambda>290$ nm is available. In the 500–750 nm region of the I_2 spectrum, the underlying continuum is overlapped with vibrational structure between 500 and 650 nm, which arises from the $B^3\Pi(0_u^+) \leftarrow X^1\Sigma_g^+$ transition (Calvert and Pitts, 1966; Okabe, 1978).

The last study to report I_2 spectral data (extinction coefficients) was that of Tellinghuisen (1973). Figure 3 shows the cross-section from our study at a resolution of 4 cm^{-1} plotted against the values calculated from the data of Tellinghuisen measured at 2.6 nm resolution and reported at 10 nm wavelength intervals. The difference in res-

© EGU 2004

olution makes direct comparison of values difficult. Nevertheless, the results show a relatively good agreement in the region from 570 to 630 nm, whereas below 570 nm, our values are significantly higher (27% higher at 500 nm). In the study of Tellinghuisen, measurements were made at room temperature (295–300 K) and with no added bath gas. In addition, the extinction coefficients from 510–620 nm were determined by extrapolating to zero pressure.

The effect of ambient pressure on the absorption spectrum of I_2 has been treated in a number of studies (Rabinowitch and Wood, 1936a; Goy and Pritchard, 1964; Ogryzlo and Thomas, 1965). These investigations demonstrated that as the total gas pressure is raised (at constant I_2 vapour pressure), absorption of I_2 in the structured region from 500 to 570 nm initially increases before levelling off at a pressure of about 500 Torr. Our cross-section value at and below the convergence limit of 499 nm agrees to within 10% of that calculated from Fig. 2 of the study of Rabinowitch and Wood, which was determined under comparable temperature-pressure conditions. This study, along with that of Ogryzlo and Thomas (1965), concluded that, as a result of pressure broadening in the structured region of the spectrum, the high pressure spectral profile of I_2 is the “true” profile in terms of the extinction coefficient (absorption cross-section) data. Consequently, the difference in experimental pressure conditions between our work and that of Tellinghuisen is likely to be responsible for the higher cross-section values determined in our study.

3.2. Photolysis rate measurements

Figure 4 illustrates the I_2 concentration measured downstream of the photolysis cell (see Fig. 1), as a function of time. The photolysis rate was determined from the following sequence of steps. Initially, $[I_2]$ was measured with no O_3 in the cell and the photolysis lamp blocked. When the O_3 was then turned on, the dark (thermal) reaction of I_2 with O_3 ($k_{295\,K}=3.8\times10^{-18}$ cm^3 molecule^{-1} s^{-1}; Vikis and MacFarlane, 1985) proceeded until a (lower) steady-state $[I_2]$ was reached (at 30–45 s). This concentration is termed $[I_2]_0$ below. The next step was to unblock the photolysis light (at 60 s) and irradiate the cell. The photo-oxidation of I_2 with O_3 was then monitored over a 3-min period, with $[I_2]$ reaching a new steady state (at 75–90 s).

The observed changes in absorption at 546 nm in the downstream absorption cell are the result of both I_2 photolysis and extinction by particles generated from condensation of the iodine oxide products in the photolysis cell (Cox and Coker, 1983; Vikis and MacFarlane, 1985; Jimenez et al., 2003; Burkholder et al., 2004). In order to correct for particle extinction, measurements under dark and light reaction conditions were also taken at three other Hg lamp emission lines (365, 405 and 436 nm), where absorption by I_2 and O_3 is negligible. The absorption dependencies for the dark and light reactions were found to vary as λ^{-6} and λ^{-5}, respectively. These data were extrapolated to fit the particle absorption at 546 nm and the initial absorption measurements (due to I_2+ particles) corrected accordingly. Particle absorption at 546 nm was found to be significant in both cases (30–35% of the total measured absorption for the dark reaction, and 80–90% when photolysis of I_2 occurred).

The rate at which I_2 is removed from the reaction cell as a result of photolysis ($I_2+h\nu \rightarrow I+I$) is described by the first-order expression

$$\frac{d[I_2]}{dt}=-J(I_2)\times[I_2], \tag{1}$$

which integrates to give

$$[I_2]_t=[I_2]_0\times\exp(-J(I_2)\times t), \tag{2}$$

where $[I_2]_t$ is the concentration at time (t), $[I_2]_0$ is the initial concentration and $J(I_2)$ is the first-order rate of photolysis.

$J(I_2)$ values were calculated from Eq. (3) by taking $[I_2]_0$ as the dark reaction steady-state concentration, and $[I_2]_t$ as the steady-state concentration after the I_2 had been irradiated for τ=12.5±2.5 s (the residence time in the photolysis cell):

$$J(I_2)=\ln\left(\frac{[I_2]_0}{[I_2]_t}\right)\times\frac{1}{\tau}. \tag{3}$$

Title Page
Abstract Introduction
Conclusions References
Tables Figures
◀| |▶
◀ ▶
Back Close
Full Screen / Esc
Print Version
Interactive Discussion

© EGU 2004

Figure 4 shows five data sets measured with an irradiance of 1350 $\mathrm{W\,m^{-2}}$ (~1 solar constant), from which a mean value for $J(I_2)$ of $0.14\pm0.04\,\mathrm{s^{-1}}$ is obtained.

Measurements were made at different irradiances in order to establish the variation of photolysis rate with light intensity (Fig. 5). The data shows a linear fit with a slope of $(1.10\pm0.07)\times10^{-4}\,\mathrm{s^{-1}\,W^{-1}\,m^{2}}$. A cloud free sky solar irradiance at the Earth's surface of 1100 $\mathrm{W\,m^{-2}}$ (assuming 20% attenuation by atmospheric absorption – Houghton, 2002), yields $J(I_2)=0.12\pm0.03\,\mathrm{s^{-1}}$ for an overhead sun.

The total rate of photolysis of I_2 can also be computed from the relation

$$\begin{aligned} J(\lambda) &= \int_\lambda F(\lambda)\times\sigma(\lambda)\times\varphi(\lambda)\,d\lambda \\ &= \int_\lambda j(\lambda)\,d\lambda, \end{aligned} \tag{4}$$

where $F(\lambda)$ denotes the incident actinic flux (photons $\mathrm{cm^{-2}\,s^{-1}\,nm^{-1}}$), $\sigma(\lambda)$ is the absorption cross-section ($\mathrm{cm^2\,molecule^{-1}}$) and $\phi(\lambda)$ is the quantum yield for photo-dissociation ($0<\phi(\lambda)<1$). $\phi(\lambda)$ for I_2 was set at a value of 1 for $290<\lambda<499$ nm and for $651<\lambda<750$ nm. In the structured region of the spectrum ($500<\lambda<650$ nm), competing fluorescence ($I_2^*+M\rightarrow I_2+M+hv$) can reduce the photo-dissociation yield from unity (Okabe, 1978). At low ambient gas pressure, the quantum yield in this region was reported as a function of wavelength by Brewer and Tellinghuisen (1972) such that $\phi_{\mathrm{min}}=0.33$ at 590 nm. However at high pressure (>150 Torr), collisional quenching of excited I_2 molecules (R2a) leads exclusively to dissociation to I atoms (Rabinowitch and Wood, 1936b). Therefore for our calculations, $\phi(\lambda)$ was set at a value of 1 across the whole spectrum. Using the measured $\sigma(\lambda)$ from this study (Fig. 2) and extraterrestrial actinic flux $F_0(\lambda)$ from the SOLAR2000 irradiance model (Tobiska et al., 2000), corrected for atmospheric absorption, $j(I_2)$ values with respect to the troposopheric boundary layer were calculated at a resolution of 1 nm (Fig. 6). Integration of the area under this plot gives a total $J(I_2)=0.15\pm0.03\,\mathrm{s^{-1}}$ for an overhead sun. This estimate is in satisfactory agreement with the measured value above.

A two-stream radiation scheme (Thompson, 1984) was used to determine the rate of photolysis of I_2 in the MBL as a function of solar zenith angle (SZA). Values corresponding to cloud-free conditions, were determined for early August (Julian Day 214) at Mace Head on the west coast of Ireland (53°20′ N). This location and time-of-year correspond to the reported observations of I_2 (Saiz-Lopez and Plane, 2004). Much of the work into iodine oxide particle production has also been carried out at this site (O'Dowd et al., 2002b). Using our measured absorption cross-section, $J(I_2)=0.17\,s^{-1}$ at midday (SZA=36°) for a zero surface albedo. For a typical water surface albedo of 0.1, $J(I_2)$ increases to $0.20\,s^{-1}$.

Hough (1988) showed that for clear-sky conditions at an altitude of 0.5 km, the variation between the photolysis rate of a species and the SZA can be described by:

$$J\,(\mathrm{SZA}) = L\cos(\mathrm{SZA})^{M} \times \exp\left(-N\sec(\mathrm{SZA})\right) \tag{5a}$$

$$\text{or for SZA} = 0, \quad J_{\max} = L \times \exp(-N)\,, \tag{5b}$$

where L, M and N are parameters calculated by convoluting the absorption cross-section and quantum yield of a species with the solar actinic flux data, determined either by direct measurement using spectro-radiometry or calculated by radiative transfer modelling. Equation (5) has been used to generate J values for a number of volatile organic species (VOC's) found in the troposphere (Jenkin et al., 1997) and more recently with respect to halogen-containing molecules including I_2, Br_2 and Cl_2 (Kanaya et al., 2003). We have therefore fitted Eq. (5) to the clear-sky data obtained from the two-stream radiation code, yielding values of $L=0.223$, $M=0.002$ and $N=0.205$ for a zero surface albedo. Figure 7 illustrates that Eq. (5) provides a very satisfactory parameterisation of $J(I_2)$ for SZA<80°. For a surface albedo of 0.1, $L=0.252$, $M=0.002$ and $N=0.185$. Also shown in Fig. 7 is the variation in the photolysis rate calculated using the parameters given by Kanaya et al. (2003), which predicts $J(I_2)=0.15\,s^{-1}$ at a SZA of 36°. The differences observed in the two plots most likely result from our higher measured absorption cross-section, compared to the lower resolution, low pressure data of Tellinghuisen (1973) used by Kanaya et al.

© EGU 2004

The photolysis rates were calculated for Cl_2 and Br_2 using the data from Kanaya et al. (2003). Table 1 lists these values along with other parameters which clearly show the trends from $Cl_2 \rightarrow Br_2 \rightarrow I_2$. Decreasing bond energies, increasing absorption cross-sections and the shift of peak absorption to the visible region of the solar spectrum lead to an increase in J values. Finally, Fig. 8 summarises the convoluted photolysis rate constants as a function of wavelength for a number of gas-phase species which release atomic iodine upon photolysis in the MBL. The integrated J values (290 nm$<\lambda<$750 nm) are (s^{-1}): 8.0×10^{-3} (CH_2I_2), 4.6×10^{-5} (CH_3I), 4.5×10^{-4} (CH_2ClI), 1.1×10^{-3} (CH_2BrI), 5.7×10^{-3} (HOI) and 0.15 (I_2).

4. Conclusions

A new measurement of the absolute absorption cross-section for I_2 over the wavelength range from 182 to 750 nm is reported for the conditions of 295 K and 760 Torr. We report a maximum absorption cross-section in the actinic wavelength range of $\sigma=(4.84\pm0.60)\times10^{-18}$ cm^2 molecule^{-1} at $\lambda=533.0$ nm. The I_2 cross-section was measured at a resolution suitable for DOAS field measurements, and is provided as supplementary material to this paper.

The rapid photolysis of I_2 in the lower atmosphere (lifetime=5–10 s for an overhead sun) results from the strong absorption of visible wavelengths (400$<\lambda<$700 nm) which penetrate down to the troposphere. Photolysis is therefore almost certainly the major loss process for I_2 in the MBL during daytime, leading to the formation of iodine oxide aerosol and causing significant O_3 depletion in the MBL (Saiz-Lopez and Plane, 2004).

Supplementary material

The I_2 absorption cross-section from 182–750 nm reported in this study is available in spreadsheet format.

© EGU 2004

Acknowledgements. This work was supported by the UK Natural Environment Research Council. The authors wish to thank G. McFiggans for helpful discussions on the use of the radiation transfer model, and T. Vondrak for providing the SOLAR2000 actinic flux data.

References

Baxter, G. P., Hickey, C. H., and Holmes, W. C.: The vapour pressure of iodine, J. Am. Chem. Soc., 29, 127–136, 1907.

Baxter, G. P. and Grose, M. R.: The vapour pressure of iodine between 50° and 95°, J. Am. Chem. Soc., 37, 1061–1072, 1915.

Bloss, W. J., Rowley, D. M., Cox, R. A., and Jones, R. L.: Kinetics and products of the IO self-reaction, J. Phys. Chem., 105, 7840–7854, 2001.

Brewer, L. and Tellinghuisen, J.: Quantum yield for unimolecular dissociation of I_2 in visible absorption, J. Chem. Phys., 56, 3929–3938, 1972.

Burkholder, J. B., Curtius, J., Ravishankara, A. R., and Lovejoy, E. R.: Laboratory studies of the homogeneous nucleation of iodine oxides, Atmos. Chem. Phys., 4, 19–34, 2004.

Calvert, J. G. and Pitts, J. N.: Photochemistry, Wiley, New York, 1966.

Carpenter, L. J., Sturges, W. T., Penkett, S. A., Liss, P. S., Alicke, B., Hebestreit, K., and Platt, U.: Short-lived alkyl iodides and bromides at Mace Head, Ireland: links to biogenic sources and halogen oxide production, J. Geophys. Res., 104, 1679–1689, 1999.

Carpenter, L. J., Hebestreit, K., Platt, U., and Liss, P. S.: Coastal zone production of IO precursors: A 2-dimensional study, Atmos. Chem. Phys., 1, 9–18, 2001.

Carpenter, L. J.: Iodine in the marine boundary layer, Chem. Rev., 103, 4953–4962, 2003a.

Carpenter, L. J., Liss, P. S., and Penkett, S. A.: Marine organohalogens in the atmosphere over the Atlantic and Southern oceans, J. Geophys. Res., 108, 4256, doi:10.1029/2002JD002769, 2003b.

Chase Jr., M. W.: NIST JANAF Thermochemical Tables, Fourth Edition, J. Phys. Chem. Ref. Data, Monograph 9, 1998.

Chatfield, R. B. and Crutzen, P. J.: Are there interactions of iodine and sulfur species in marine air photochemistry?, J. Geophys. Res., 95, 22 319–22 341, 1990.

Cox, R. A. and Coker, G. B.: Absorption cross-section and kinetics of IO in the photolysis of CH_3I in the presence of ozone, J. Phys. Chem., 87, 4478–4484, 1983.

CRC Handbook of Chemistry and Physics, 82nd Edition, CRC Press, Boca Raton, 2001–2002.

Davis, D., Crawford, J., Liu, S., McKeen, S., Bandy, A., Thornton, D., Rowland, F., and Blake, D.: Potential impact of iodine on tropospheric levels of ozone and other critical oxidants, J. Geophys. Res., 101, 2135–2147, 1996.

DeMore, W. B., Sander, S. P., Golden, D. M., Hampson, R. F., Kurylo, M. J., Howard, C. J., Ravishankara, A. R., Kolb, C. E., and Molina, M. J.: Chemical kinetics and photochemical data for use in stratospheric modelling: Evaluation Number 12, JPL Publ., 97–4, 1997.

Garland, J. A. and Curtis, H.: Emission of iodine from the sea surface in the presence of ozone, J. Geophys. Res., 86, 3183–3186, 1981.

Goy, C. A. and Pritchard, C. A.: Pressure dependence of the visible iodine bands, J. Mol. Spectrosc., 12, 38–44, 1964.

Hoffmann, T., O'Dowd, C. D., and Seinfeld, J. H.: Iodine oxide homogeneous nucleation: An explanation for coastal new particle production, Geophys. Res. Lett., 28, (10), 1949–1952, 2001.

Hough, A. M.: The calculation of photolysis rates for use in global tropospheric modelling studies, AERE Report R-13259 (HMSO), London, 1988.

Houghton, J.: The physics of atmospheres, 3rd Edition, Cambridge Uni. Press, Cambridge, 2002.

International union of pure and applied chemistry (IUPAC): subcommittee for gas kinetic data evaluation, http://www.iupac-kinetic.ch.cam.ac.uk.

Jenkin, M. E., Cox, R. A., and Candeland, D. E.: Photochemical aspects of tropospheric iodine behaviour, J. Atmos. Chem., 2, (4), 359–375, 1985.

Jenkin, M. E., Saunders, S. M., and Pilling, M. J.: The tropospheric degradation of volatile organic compounds: a protocol for mechanism development, Atmos. Env., 31, 81–104, 1997.

Jimenez, J. L., Bahreini, R., Cocker III, D. R., Zhuang, H., Varutbangkul, V., Flagan, R. C., Seinfeld, J. H., O'Dowd, C. D., and Hoffmann, T.: New particle formation from photooxidation of diiodomethane (CH_2I_2), J. Geophys. Res., 108, D10, 4318, doi:10.1029/2002JD002452, 2003.

Kanaya, Y., Kajii, Y., and Akimoto, H.: Solar actinic flux and photolysis frequency determinations by radiometers and a radiative transfer model at Rishiri Island: comparisons, cloud effects and detection of an aerosol plume from Russian forest fires, Atmos. Env., 37, 2463–2475, 2003.

McFiggans, G., Plane, J. M. C., Allan, B. J., Carpenter, L. J., Coe, H., and O'Dowd, C.: A

© EGU 2004

modeling study of iodine chemistry in the marine boundary layer, J. Geophys. Res., 105, 14 371–14 385, 2000.

McFiggans, G., Cox, R. A., Mössinger, J. C., Allan, B. J., and Plane, J. M. C.: Active chlorine release from marine aerosols: Roles for reactive iodine and nitrogen species, J. Geophys. Res., 107, D15, 4271, doi:10.1029/2001JD000383, 2002.

Mäkelä, J. M., Hoffmann, T., Holzke, C., Väkevä, M., Suni, T., Mattila, T., Aalto, P. P., Tapper, U., Kaupinnen, E. I., and O'Dowd, C. D.: Biogenic iodine emissions and identification of end-products in coastal ultrafine particles during nucleation bursts, J. Geophys. Res., 107, D19, 8110, doi:10.1029/2001JD000580, 2002.

Miyake, Y. and Tsunogai, S.: Evaporation of iodine from the ocean, J. Geophys. Res., 68, 3989–3993, 1963.

O'Dowd, C. D., Jimenez, J. L., Bahreini, R., Flagan, R. C., Seinfeld, J. H., Hameri, K., Pirjola. L., Kulmala, M., Jennings, S. G., and Hoffmann, T.: Marine aerosol formation from biogenic iodine emissions, Nature, 417, 632–636, 2002a.

O'Dowd., C. D., Hämeri, K., Mäkelä, J. M., Pirjola, L., Kulmala, M., Gerard Jennings, S., Berresheim, H., Hansson, H.-C., de Leeuw, G., Kunz, G. J., Allen, A. G., Hewitt, C. N., Jackson, A., Viisanen, Y., and Hoffmann, T.: A dedicated study of new particle formation and fate in the coastal environment (PARFORCE): Overview of objectives and achievements, J. Geophys. Res., 107, D19, 8108, doi:10.1029/2001JD000555, 2002b.

Ogryzlo, E. A. and Thomas, G. E.: Pressure dependence of the visible absorption bands of molecular iodine, J. Mol. Spectrosc., 17, 198–202, 1965.

Okabe, H.: Photochemistry of small molecules, John Wiley & Sons, New York, 1978.

Rabinowitch, E. and Wood, W. C.: The extinction coefficients of iodine and other halogens, Trans. Faraday Soc., 32, 540–546, 1936a.

Rabinowitch, E. and Wood, W. C.: Dissociation of excited iodine molecules, J. Chem. Phys., 4, 358–362, 1936b.

Saiz-Lopez, A. and Plane, J. M. C.: Novel iodine chemistry in the marine boundary layer, Geophys. Res. Lett., 31, L04112, doi:10.1029/2003GL019215, 2004.

Shirley, D. A. and Giauque, W. F.: The entropy of iodine, Heat capacity from 13 to 327 K, Heat of sublimation, J. Am. Chem. Soc., 81, 4778–4779, 1959.

Solomon, S., Garcia, R. R., and Ravishankara, A. R.: On the role of iodine in ozone depletion, J. Geophys. Res., 99, 20 491–20 499, 1994.

Tellinghuisen, J.: Resolution of the visible-infrared absorption spectrum of I_2 into three contributing transitions, J. Chem. Phys., 58, 2821–2834, 1973.

Thompson, A. M.: The effect of clouds on photolysis rates and ozone formation in the unpolluted troposphere, J. Geophys. Res., 89, 1341–1349, 1984.

Tobiska, W. K., Woods, T., Eparvier, F., Viereck, R., Floyd, L., Bouwer, D., Rottman, G., and White, O. R.: The SOLAR2000 empirical solar irradiance model and forecast tool, J. Atmos. Solar-Terr. Phys., 62, 1233–1250, 2000.

Vikis, A. C. and MacFarlane, B.: Reaction of iodine with ozone in the gas phase, J. Phys. Chem., 89, 812–815, 1985.

Vogt, R., Sander, R., Von Glasow, R., and Crutzen, P. J.: Iodine chemistry and its role in halogen activation and ozone loss in the marine boundary layer: A model study, J. Atmos. Chem., 32, 375–395, 1999.

Title Page
Abstract Introduction
Conclusions References
Tables Figures
◀▮ ▶▮
◀ ▶
Back Close
Full Screen / Esc
Print Version
Interactive Discussion

© EGU 2004

Table 1. Trends in properties of the halogen diatomics.

Halogen (X_2)	**Bond Energy**[a] **(kJ mol^{-1})**	$(10^{20})\sigma_{max}$ **($cm^2 molecule^{-1}$)**	λ_{max} **(nm)**	J **(s^{-1})**
Cl_2	243	26[b]	330[b]	0.0022[c]
Br_2	193	68[b]	420[b]	0.034[c]
I_2	151	484[d]	533[d]	0.18[e]

[a] at 298 K (CRC Handbook of Chemistry & Physics, 2001).
[b] at 298 K, from the IUPAC gas kinetic database.
[c] values calculated for SZA=0 using parameters given in Kanaya et al. (2003).
[d] measured in this study.
[e] from this study for SZA=0.

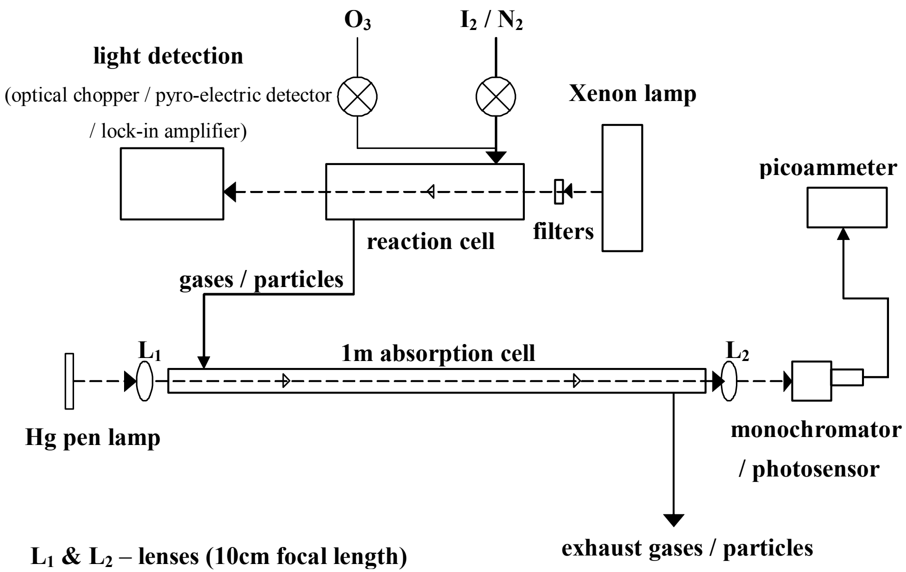

Fig. 1. Schematic of the optical absorption experiment used to measure the rate of photolysis of I_2.

© EGU 2004

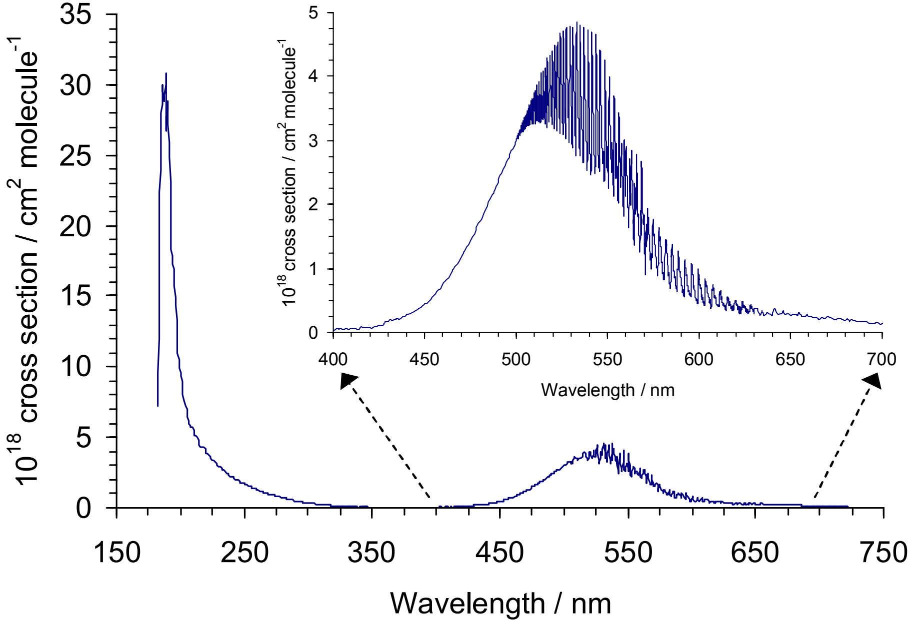

Fig. 2. Measured I_2 absorption cross-section profile (full range – 1 nm interval) with visible region (400–700 nm) expanded at higher resolution (4 cm^{-1}) to show the detailed vibrational structure from 500–650 nm.

Title Page
Abstract Introduction
Conclusions References
Tables Figures
◀◀ ▶▶
◀ ▶
Back Close
Full Screen / Esc
Print Version
Interactive Discussion

© EGU 2004

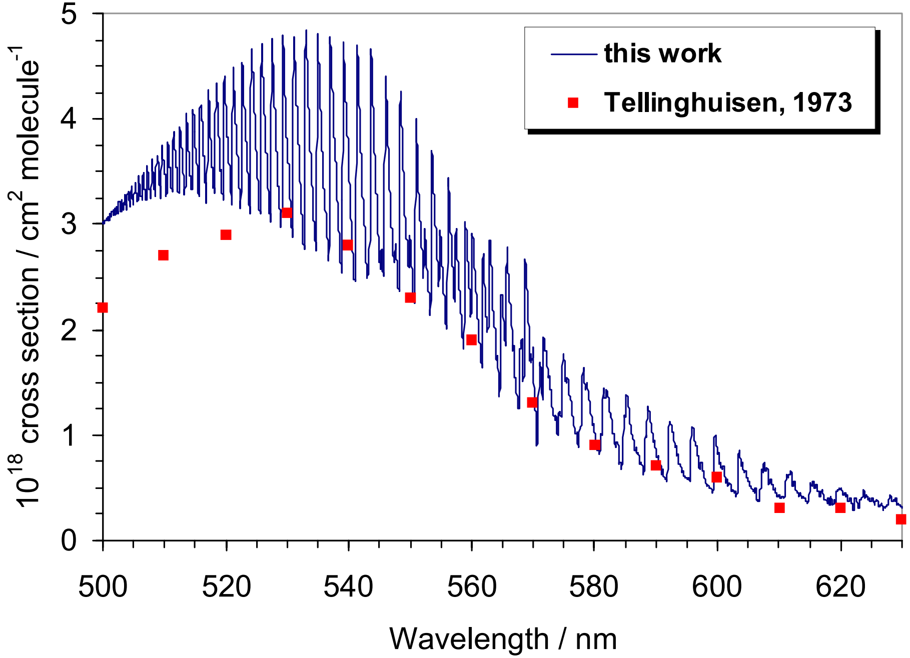

Fig. 3. Comparison of the high resolution I_2 spectrum (500–630 nm) from this study with the values calculated using the data from Tellinghuisen (1973).

© EGU 2004

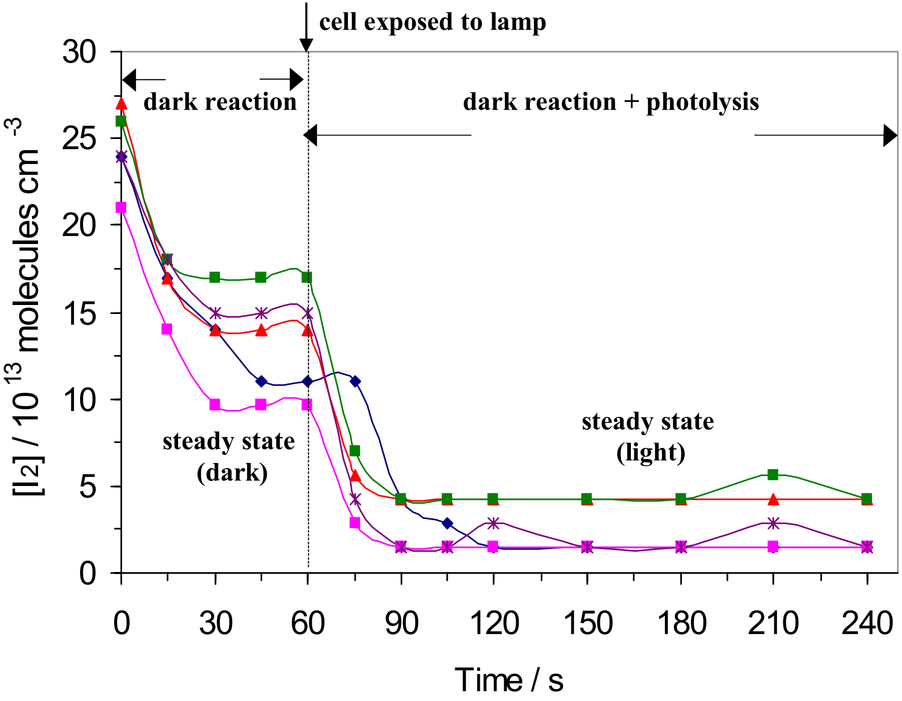

Fig. 4. Data sets for I_2+O_3 photo-oxidation at a cell irradiance of 1350 Wm^{-2}. The different symbols refer to individual experimental runs under the same conditions.

© EGU 2004

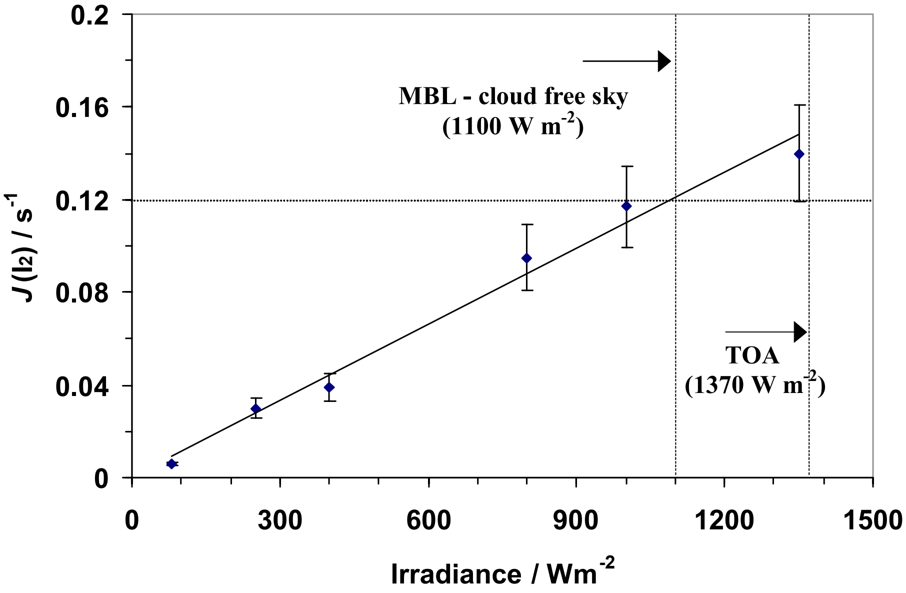

Fig. 5. Variation of the laboratory measured rate of I_2 photolysis with light irradiance. Data points shown correspond to the mean values calculated from 5 experiments run for each light irradiance value, all other reaction parameters being identical (error bars represent standard deviation in individual measurements). TOA (top of atmosphere) irradiance = 1 solar constant.

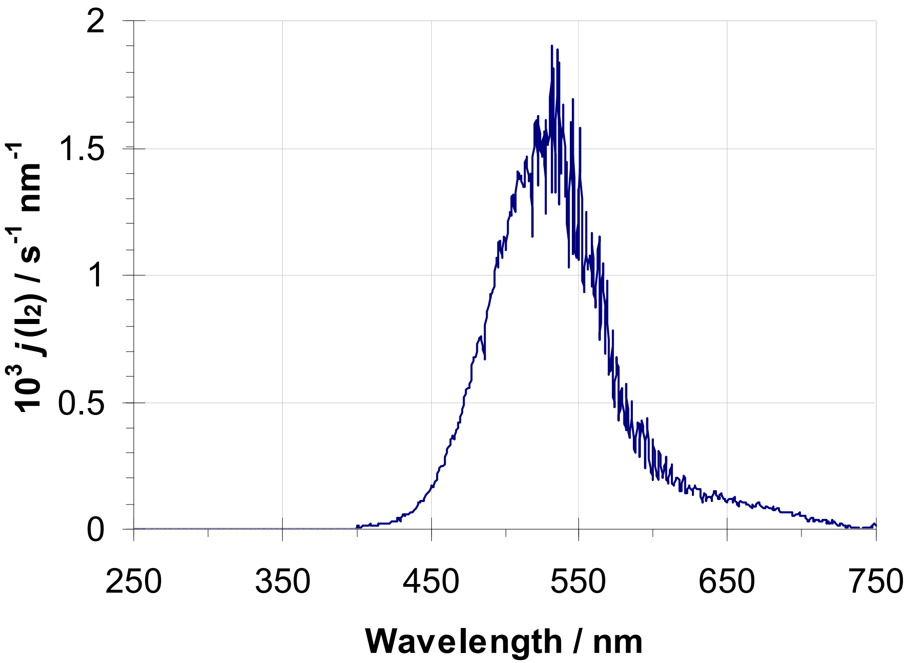

Fig. 6. Wavelength dependence of the I_2 photolysis rate in the lower atmosphere, calculated at 1 nm resolution. Values were convoluted using the measured I_2 cross-section, solar flux data from Tobiska et al. (2000) (attenuated by atmospheric absorption) and a photo-dissociation yield of unity.

© EGU 2004

© EGU 2004

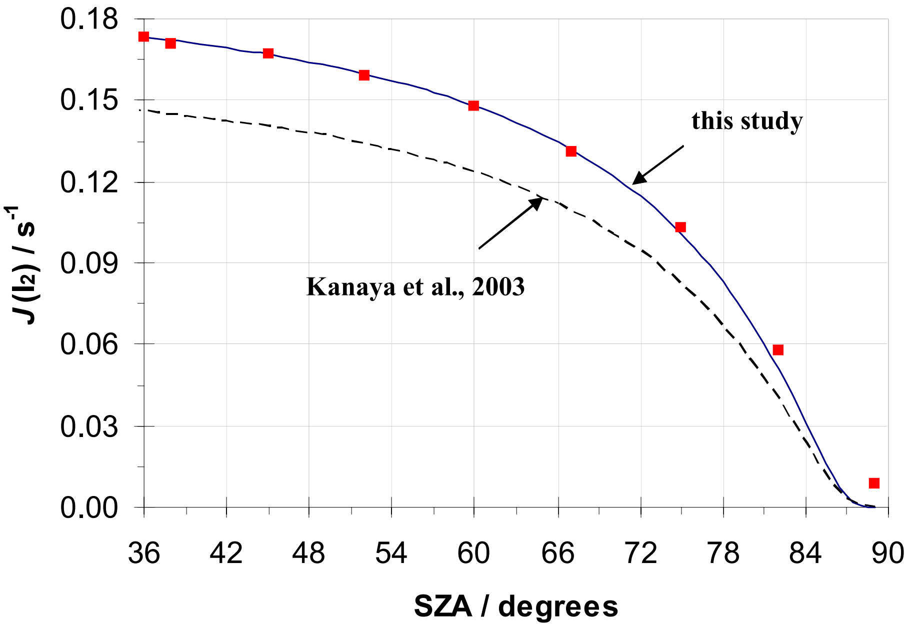

Fig. 7. Variation of $J(I_2)$ with SZA. Values were calculated for a mid-latitude location (53° N) in early August under cloud free conditions. The discrete data points are from the two-stream radiation model (Thompson, 1984), the solid line is the fit to these points using Eq. (5) with L=0.223, M=0.002 and N=0.205 (see text) and the dashed line is the data calculated for L=0.1912, M=0.0019 and N=0.2185 (Kanaya et al., 2003).

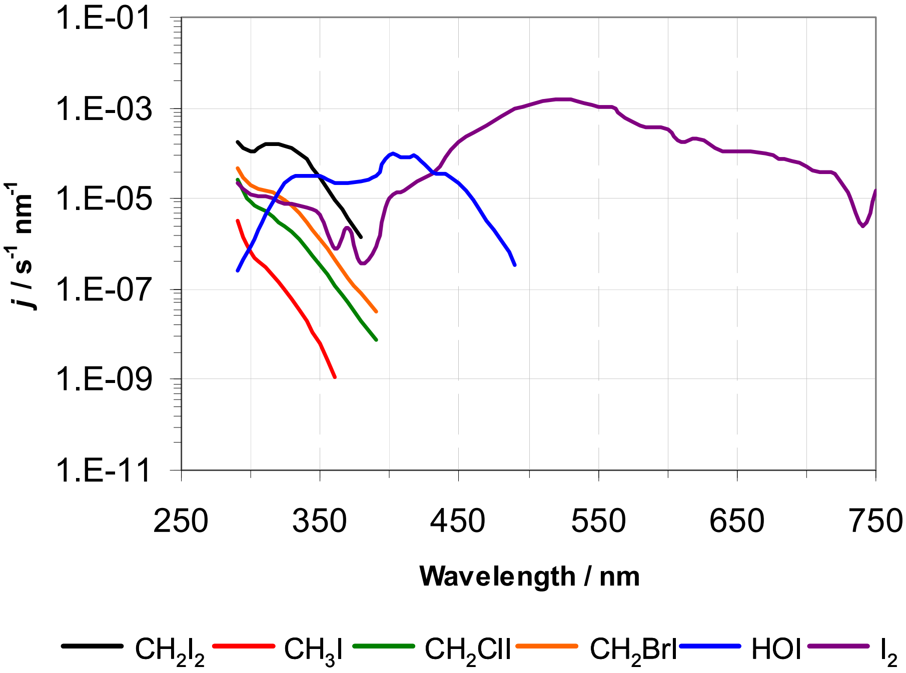

Fig. 8. Convoluted tropospheric photolysis rate variation (clear sky, overhead sun) for a number of iodine-containing species (absorption cross-sections at 10 nm intervals). Cross-section data was taken from the IUPAC gas kinetic database (with the exception of I_2 for which our measured values were used), the photo-dissociation quantum yields were set to unity for all species, and direct actinic fluxes calculated from top of atmosphere data (corrected for atmospheric absorption). Integration across the wavelength range gives the photolysis rate constant (*J*) for each species (see text for values).

© EGU 2004